

# Ibn Al-Haitham Journal for Pure and Applied Sciences

Journal homepage: jih.uobaghdad.edu.iq PISSN: 1609-4042, EISSN: 2521-3407 IHJPAS. 2025, 38(4)



# Neutron Halo Structure of Unstable Exotic <sup>14</sup>B and <sup>18</sup>N Nuclei

Moath S. Hamad<sup>1\*</sup> and Ahmed N. Abdullah<sup>2</sup> ■

<sup>1,2</sup> Department of Physics, College of Science, University of Baghdad, Baghdad, Iraq.
\*Corresponding Author.

Received: 21 April 2025 Accepted: 24 July 2025 Published: 20 October 2025

doi.org/10.30526/38.4.4147

#### **Abstract**

The ground-state properties like the nuclear densities and the root mean square (rms) radii for exotic neutron-rich nuclei  $^{14}$ B and  $^{18}$ N have been investigated using the Skyrme Hartree-Fock and Bear-Hodgson calculations to study the structure of these nuclei. The results of the evaluation are contrasted with the experimental data that is currently available. It found that a common feature of the neutron and matter densities for the above-selected exotic nuclei is the long tail behavior. We assumed that both  $^{14}$ B and  $^{18}$ N have a structure of the core nuclei  $^{13}$ B and  $^{17}$ N plus a valence neutron. It found that the structure of the valence one-neutron of  $^{14}$ B and  $^{18}$ N is a pure  $2s_{1/2}$  Configuration. The elastic charge form factors of the above selected exotic nuclei are evaluated using the plane wave Born approximation and compared with those of their stable isotope  $^{10}$ B and  $^{14}$ N.

**Keywords:** Exotic nuclei, Elastic form factors, Bear-Hodgson, The Skyrme-Hartree-Fock.

# 1. Introduction

The study on the structure of short-lived nuclei far from  $\beta$ -stability has become a hot point in nuclear physics due to its exotic properties (1-4). The resulting discovery of neutron halo in certain anomalous light neutron-rich nuclei was in  ${}^{6}\text{He}$ ,  ${}^{11}\text{Li}$ ,  ${}^{11}\text{Be}$ ,  ${}^{14}\text{Be}$ ,  ${}^{19}\text{C}$ , etc (5-7). The nuclear halo is a quantum effect that arises from the very weak binding of the valence nucleons and their occupation on the orbits with l=0, 1 (low angular momentum), which allows the wave function of these valence nucleons to take on an extended radial dimension (8). The primary characteristic of the nuclear-matter density distribution in halo nuclei is the presence of a low-density tail at vast radial distances (9).

The information about such nuclear structure can be extracted from the fragment momentum distribution of fragmentation reaction, total reaction cross section, Coulomb dissociation, and quadrupole moment (10, 11). Additional information on the nuclear structure can be obtained by the proton elastic scattering at intermediate energies. It gives insights into both the nuclear-matter density distribution and the nuclear-matter radius (12). This technique is well-established for the study of stable nuclei and may also be used to investigate unstable nuclei when applied to inverse kinetics with radiation beams. The methodology has been effectively utilized to examine the isotopic <sup>12,14</sup>Be (9) and <sup>8,9,11</sup>Li (13).

The two-body (Core + n) and three-body (Core + 2n) models utilizing wave functions of various potentials have been employed to examine the ground state characteristics, including proton, neutron, and matter densities, of several halo nuclei, like as <sup>22</sup>N, <sup>23</sup>O, <sup>14</sup>Be, and <sup>17</sup>B,

etc (14-18). Also, the associated rms radii of these exotic nuclei have been studied by these models. The calculated results have been provided for the halo structure for the considered exotic nuclei.

In this work, the characteristics of the ground state pertaining to exotic <sup>14</sup>B and <sup>18</sup>N nuclei, such as the proton  $[\rho_p(r)]$ , neutron  $[\rho_n(r)]$  and matter  $[\rho_m(r)]$ , the corresponding root mean square (rms) radii, and elastic charge form factors  $(F_{ch}(q))$ , will be investigated using the Hartree-Fock (HF) and Bear-Hodgson (BH) calculations. We will examine the reaction crosssections  $(\sigma_R)$  for that nucleus use the Kox formula (KF) and Glauber model (GM).

#### 2. Materials and Methods

The  $\rho_m(r)$  of exotic nuclei is (19):

$$\rho_m(r) = \rho_c(r) + \rho_v(r) \tag{1}$$

where  $\rho_c(r)$  (core density) and  $\rho_h(r)$  (halo density) are expressed as (19):

$$\rho_c(r) = \frac{1}{4\pi} \sum_{n\ell j} N_c^{n\ell j} \left| R_{n\ell j}(r) \right|^2 \tag{2}$$

$$\rho_h(r) = \frac{1}{4\pi} \sum_{n\ell j} N_h^{n\ell j} \left| R_{n\ell j}(r) \right|^2 \tag{3}$$

where  $R_{n\ell j}(r)$  and  $N^{n\ell j}$  denote the occupation number of the orbit  $n\ell j$ , respectively.

The  $R_{n\ell j}(r)$  taken from Schrodinger equation of this solution of radial part and using BH potential (20):

$$\frac{d^2 R_{n\ell j}(r)}{dr^2} + \frac{2m}{\hbar^2} \left[ \varepsilon_{n\ell j} - V(r) - \frac{\hbar^2}{2m} \frac{\ell(\ell+1)}{r^2} \right] R_{n\ell j}(r) = 0$$
 (4)

Where  $\varepsilon_{n\ell i}$  and the V(r) given as (21)

$$V(r) = V_0(r) + V_{so}(r) \vec{L} \cdot \vec{S} + V_c(r)$$
(5)

 $V_0(r)$  the central potential taken from following from (21):

$$V_0(r) = \frac{-V_0}{1 + \left[e^{(r - R_0)/a_0}\right]} \tag{6}$$

 $V_{so}(r)$  is the spin orbit potential (21):

$$V_{so}(r) = V_{so} \frac{1}{r} \left[ \frac{d}{dr} \frac{1}{(1 + e^{(r - R_{so})/a_{so}})} \right]$$
 (7)

 $V_c(r)$  (for protons only) is Coulomb potential (21):

$$V_c(r) = \begin{cases} \frac{Ze^2}{r} & \text{for } r > R_c \\ \frac{Ze^2}{R_c} \left[ \frac{3}{2} - \frac{r^2}{2R_c^2} \right] & \text{for } r \le R_c \end{cases}$$

$$\tag{8}$$

and  $V_c(r) = 0$  for neutrons.

$$V_0 = V_0^{n,p} \qquad for \qquad -15 < \varepsilon_{n\ell i} < 0 \tag{9}$$

The 
$$V_0$$
 is potential depth [in **Equation 6**] takes the BH form (22):  

$$V_0 = V_0^{n,p} \qquad \qquad for \qquad -15 < \varepsilon_{n\ell j} < 0 \qquad \qquad (9)$$

$$V_0 = V_0^{n,p} - \beta \left(\varepsilon_{n\ell j} + 15\right) \qquad for \qquad \varepsilon_{n\ell j} < -15 \text{ MeV}$$

The potential depth for neutrons  $(V_0^n)$  and protons  $(V_0^p)$  whereas the  $\beta$  is constant.

The Skyrme force are given by (23):

$$V_{Skyrme} = \sum_{i < j} V_{ij} = t_0 (1 + x_0 P_{\sigma}) \delta(\vec{r}) + \frac{t_1}{2} (1 + x_1 P_{\sigma}) \left[ \delta(\vec{r}) \vec{k}^2 + \vec{k}'^2 \delta(\vec{r}) \right] + t_2 (1 + x_2 P_{\sigma}) \vec{k'} \cdot \delta(\vec{r}) \vec{k} + \frac{1}{6} t_3 (1 + x_3 P_{\sigma}) \rho^{\alpha} (\vec{R}) \delta(\vec{r}) + i t_4 \vec{k'} \cdot \delta(\vec{r}) (\vec{\sigma}_i + \vec{\sigma}_j) \times \vec{k} ,$$
 (11)

 $P_{\sigma}$  represents is space operator exchange,  $\vec{\sigma}$  is the vector comprising the Pauli spin matrices  $\delta(\vec{r})$  denotes the delta function,  $\vec{k}$  indicates is relative, and  $t_0$ ,  $t_1$ ,  $t_2$ ,  $t_3$ ,  $t_4$ ,  $x_0$ ,  $x_1$ ,  $x_2$ ,  $x_3$ , and  $\alpha$  represent the parameters associated with the Skyrme force.

The charge, as well as the densities of protons or neutrons with the range of the Skyrme HF methodology, are articulated by (24):

$$\rho_{q}(\vec{r}) = \sum_{\beta \in q} w_{\beta} \psi_{\beta}^{+}(\vec{r}) \psi_{\beta}(\vec{r}), \qquad g = n, p, ch$$
 (12)

where  $\psi_{\beta}$  is the wave function of a single particle and  $w_{\beta}$  denotes the probability of occupation for the state  $\beta$ .

The nucleus charge distributions  $[\rho_{ch}(r)]$  can be obtained from the following folding relation (25):

$$\rho_{ch}(r) = \int \rho_p(r) f_p(r'-r) dr', \tag{13}$$

where  $\rho_p(r)$  and  $f_p$  are proton density.

Where  $f_p$  takes from following form of Gaussian (26):

$$f_p(r) = \frac{1}{(\sqrt{\pi}a_p)^3} e^{(-r^2/a_p^2)}$$
(14)

The core  $(R_c)$ , matter  $(R_m)$ , proton  $(R_p)$  and neutron  $(R_n)$  rms radii are obtained by (27):

$$R_g = \langle r_g^2 \rangle^{1/2} = \left[ \frac{\int r^2 \rho_g(r) dr}{\int \rho_g(r) dr} \right]^{1/2} \qquad g = c, m, n, p, ch$$
 (15)

In PWBA, the elastic charge form factor  $(F_{ch}(q))$  is given by (28):

$$F_{ch}(q) = \frac{4\pi}{Z} \int_0^\infty \rho_{ch}(r) j_0(qr) r^2 dr,$$
 (16)

The  $\sigma_R$  use the GM (29) and KF (30) given, respectively, as:

$$\sigma_R = 2\pi \int [1 - T(b)]b \, db$$
, (17)

$$\sigma_R = \pi r_0^2 \left[ A_p^{1/3} + A_t^{1/3} + a \frac{A_p^{1/3} A_t^{1/3}}{A_p^{1/3} + A_t^{1/3}} - C(E) \right]^2 \left( 1 - \frac{B_c}{E_{cm}} \right)$$
(18)

# 3. Results

The ground-state characterizes nuclear densities, and the rms radii for exotic neutron-rich nuclei  $^{14}\mathrm{B}$  and  $^{18}\mathrm{N}$  have been investigated in the framework of the HF and BH calculations. The elastic  $F_{ch}(q)$  of above selected exotic nuclei are evaluated using the PWBA. We use the KDEX Skyrme parameterization within HF calculations in this work. The values of the KDEX parameterization employed in our calculations are  $t_0=-1419.8304,\ t_1=309.1373,\ t_2=-172.9562,\ t_3=10465.3523,\ x_0=0.1474,\ x_1=-0.0853,\ x_2=-0.6144,\ x_3=0.0220,\ W_0=98.8973,\ \gamma=0.4989$  (31). The densities of both core and tail (halo) parts in HF and BH calculations are described by radial wave functions for the HF and BH potentials, respectively. We assumed that both  $^{14}\mathrm{B}$  (J $^\pi$ , T=2 $^-$ ,2) and  $^{18}\mathrm{N}$  (J $^\pi$ , T=1 $^-$ ,2) have a structure of the core nuclei  $^{13}\mathrm{B}$  (J $^\pi$ , T=3/2 $^-$ ,3/2) and  $^{17}\mathrm{N}$  (J $^\pi$ , T=1/2 $^-$ ,3/2), with configurations  $\{(1s_{1/2})^4,(1p_{3/2})^7,(1p_{1/2})^2\}$  and  $\{(1s_{1/2})^4,(1p_{3/2})^8,(1p_{1/2})^3,(1d_{5/2})^2\}$ , respectively plus valence one neutron . The valence neutron of both  $^{14}\mathrm{B}$  and  $^{18}\mathrm{N}$  is assumed to be in a pure  $2s_{1/2}$  orbit.

**Table 1** displays the values of the BH parameters utilized in the present calculations for selected nuclei. The potential depth for neutrons  $(V_0^n)$  and protons  $(V_0^p)$  in core nuclei has been used the default of the NushellX@MSU program (32) has been used, where the  $V_0^n$  for valence neutron and other parameters, provide the experimental  $\varepsilon$  of the last neutron as well as a matter (rms) radial for exotic nuclei. The parameter  $\beta$  has been fixed at a value of 0.51 (22).

**Table 1.**The BH parameters.

Nuclei	$V_0^{p,n}$ (MeV)		V <sub>so</sub> (MeV)	$a_0 = a_{so}$	$r_0 = r_{so}$	r <sub>c</sub>
	Core	Halo	V <sub>so</sub> (MeV)	fm	fm	fm
$^{14}B$	53.172	48.73	7.0	0.520	1.316	1.2
$^{18}N$	64.496	35.92	7.0	0.621	1.465	1.2
$^{10}\mathrm{B}$	55.	70	7.0	0.620	1.236	1.2
$^{14}N$	55.	70	7.0	0.620	1.236	1.2

The calculated  $\varepsilon$  for both protons and neutrons are presented in **Table 2** together with the  $\varepsilon_{exp.}$  (33) of the valence neutron.

**Table 2.**The calculated  $\varepsilon$ .

Nuclei	m 0	Pr	Proton		Neutron	
	$n\ell_j$	$V_0$ (MeV)	$\varepsilon$ (MeV)	$V_0$ (MeV)	$\varepsilon$ (MeV)	$\varepsilon_{exp.}(\text{MeV})$ (33)
<sup>14</sup> B	1s <sub>1/2</sub>	67.78	-43.676	70.13	-48.289	
<sup>18</sup> N	$1p_{3/2}$	54.89	-18.400	56.70	-21.947	
	$1p_{1/2}$			53.28	-15.223	
	$2s_{1/2}$			48.05	-0.97	-0.97
	$1s_{1/2}$	92.67	-70.285	96.09	-76.994	
	$1p_{3/2}$	79.76	-44.947	82.63	-50.589	
	$1p_{1/2}$	77.45	-40.447	80.38	-46.166	
	$1d_{5/2}$			70.17	-26.139	
	$2s_{1/2}$			35.92	-2.828	-2.828

The HF and BH calculations for the core  $(R_c)$ , matter  $(R_m)$ , proton  $(R_p)$  and neutron  $(R_n)$  rms radii (in fm) of selected halo nuclei are presented in **Tables 3** and **4**. For comparison purposes, the corresponding experiment rms radii (34-37) are also given in these tables. From these tables, we noted that the calculated results of our present study agree reasonably within the quoted error with the experimental results.

**Table 3.** The calculated  $R_c$  and  $R_m$  rms radii and experimental ones.

Nuclei	$R_c$ (fm)			$R_m$ (fm)		
	$\mathbf{HF}$	BH	<b>Exp.</b> (34)	HF	BH	Exp. (34, 35)
<sup>14</sup> B	2.42	2.44	2.46±0.12	2.89	2.77	2.77±0.04
$^{18}N$	2.57	2.57	$2.49\pm0.15$	2.87	2.80	$2.80\pm0.04$

**Table 4.** The calculated  $R_p$  and  $R_n$  rms radii and experimental ones.

Nuclei		$R_p$ (fm)			$R_n$ (fm)	
	HF	BH	Exp. (36)	HF	BH	Exp. (37)
$^{14}\mathrm{B}$	2.46	2.40	2.46±0.07	3.12	2.95	3.27±0.16
$^{18}N$	2.58	2.50		3.03	2.98	2.925±0.067

The calculated matter densities obtained by both HF (left part) and BH (right part) calculations for exotic <sup>14</sup>B and <sup>18</sup>N nuclei and core <sup>13</sup>B and <sup>17</sup>N nuclei, along with the tail (one-neutron halo) part, are shown in **Figure 1**. The blue, black, and dashed-red curves represent the core, tail part, and matter densities, respectively. The experimental matter densities for <sup>14</sup>B (38) and <sup>18</sup>N (39) are presented in this figure by a grey area for comparison. **Figure 1a** and **b** show the densities for <sup>14</sup>B, while **Figure 1c** and **d** correspond to those for <sup>18</sup>N. A common feature of the dashed-red curves, which can be shown in **Figure 1**, is the long tail behavior. Clearly, the dashed-red curves obtained with both HF and BH calculations lie within the experimental uncertainties and agree well with the experiment.

**Figure 2 a-d** summarize the calculated proton (black curve) and neutron (blue curve) densities in <sup>14</sup>B (upper panel) and <sup>18</sup>N (lower panel) obtained by the HF and BH calculations. From these figures, it can be clearly seen that the neutron densities of <sup>14</sup>B and <sup>18</sup>N have a long tail with respect to the proton densities. This means that <sup>14</sup>B and <sup>18</sup>N are neutron-halo nuclei. **Figure 3a-d** compare the calculated results of matter densities for unstable <sup>14</sup>B and <sup>18</sup>N (dashed red distributions) and stable <sup>10</sup>B and <sup>14</sup>N (blue distributions) isotopes. From these figures, we can observe that, there is a difference in the behavior of the blue and dashed red distributions. This demonstrates a long tail in dashed red distributions and supports the halo structure of <sup>14</sup>B and <sup>18</sup>N nuclei.

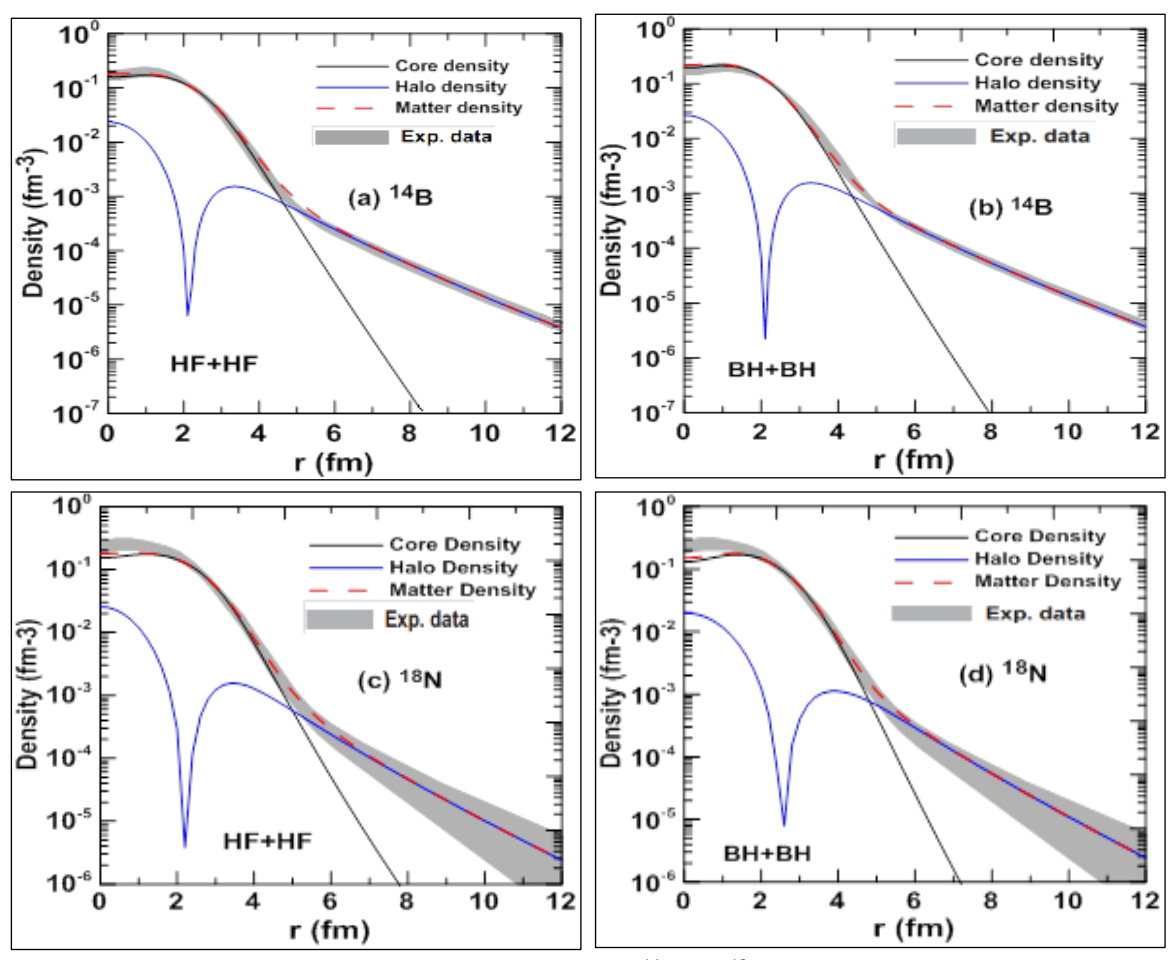


Figure 1. The matter, core and halo density for halo nuclei <sup>14</sup>B and <sup>18</sup>N.

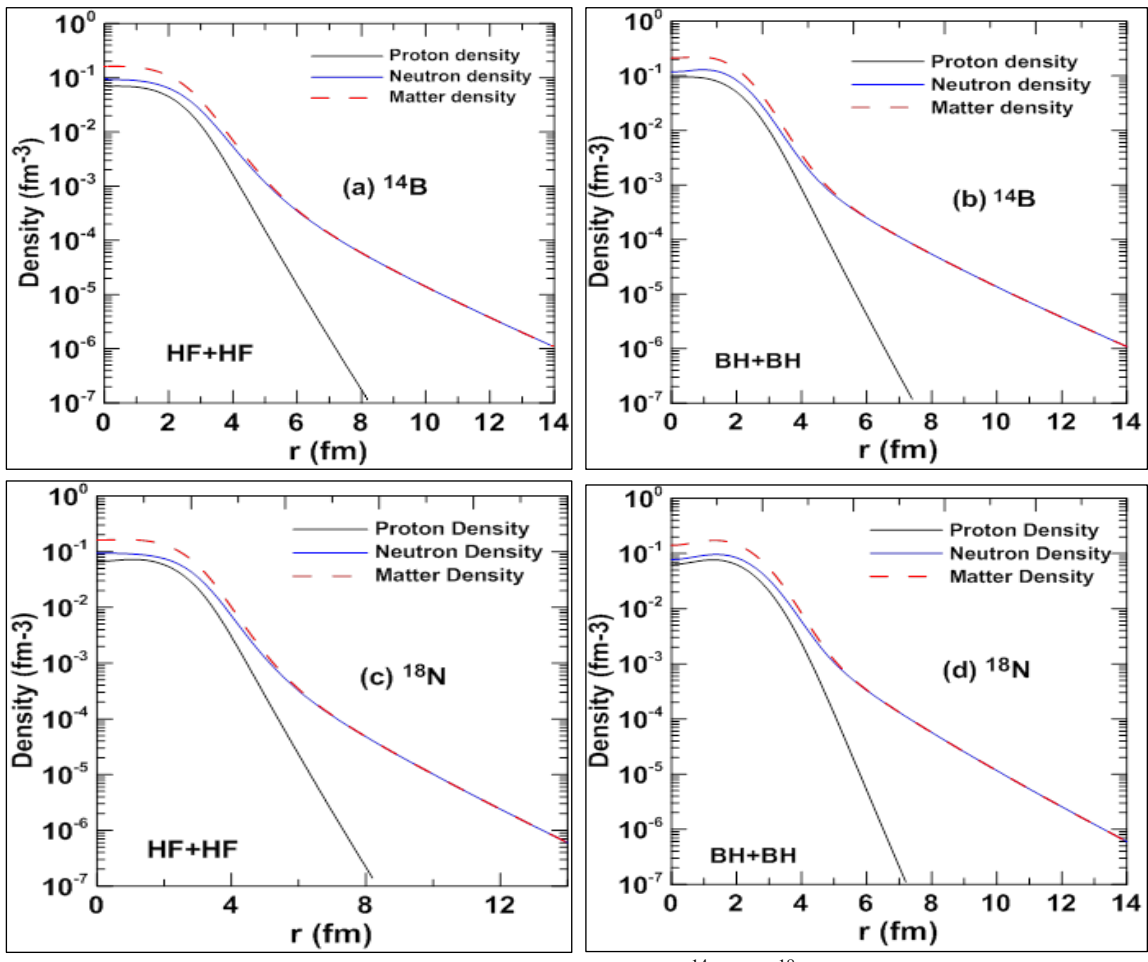
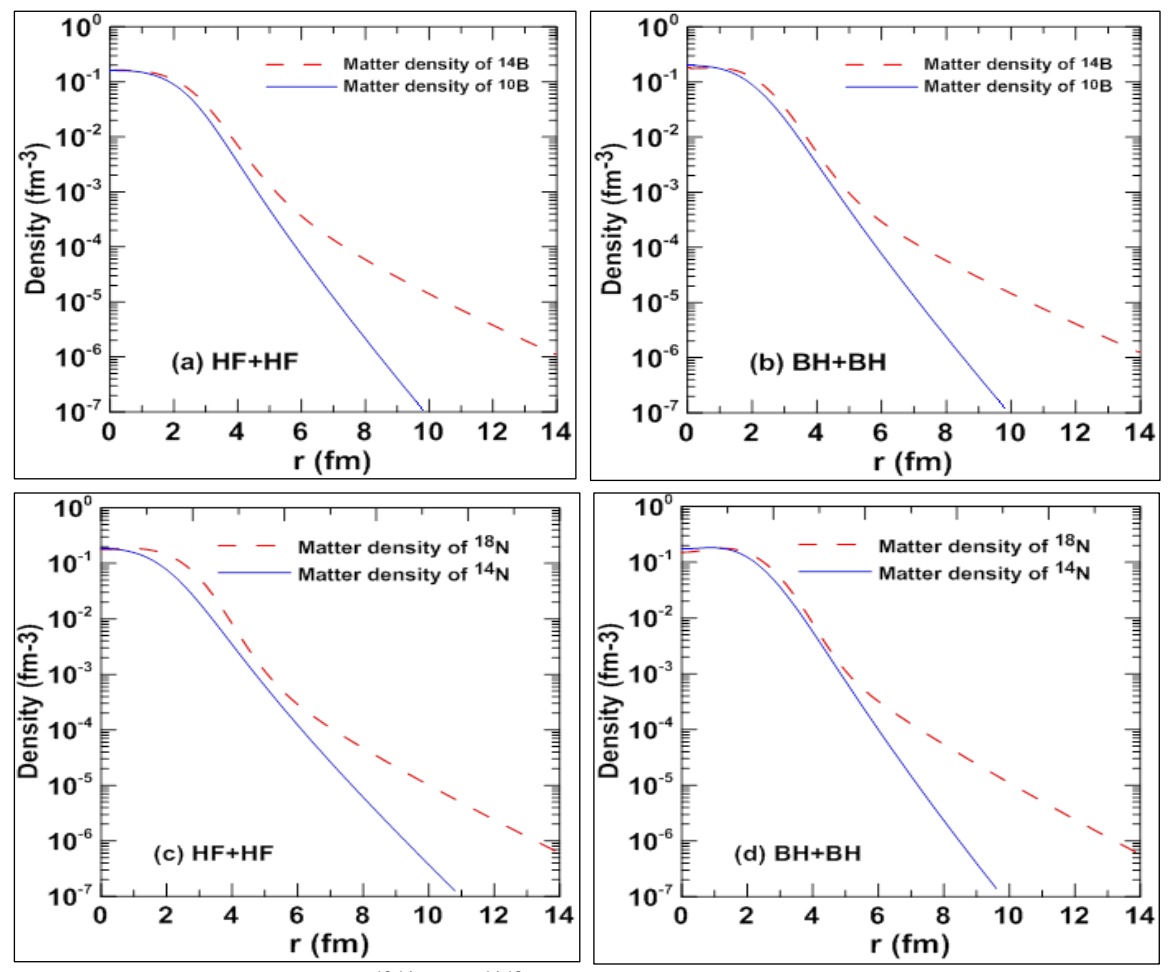


Figure 2.The matter, proton and neutron density for halo nuclei <sup>14</sup>B and <sup>18</sup>N.



**Figure 3**. The matter for isotopes <sup>10,14</sup>B and <sup>14,18</sup>N.

**Figure 4a-d** depicted the results of the longitudinal form factors (C0+C2) of  $^{10,14}$ B (upper panel) and  $^{14,18}$ N (bottom panel) isotopes calculated by HF and BH calculations. Therein, the blue and red curves refer to C0+C2 of unstable and stable isotopes, respectively. While the calculated results of C0 and C2 for unstable  $^{14}$ B and  $^{18}$ N nuclei are given by the dashed and black curves, respectively. For comparison the experimental  $F_{ch}(q)$  for stable isotopes  $^{10}$ B (40) and  $^{14}$ N (41) are given by dotted symbols. The agreement is shown to be very well between the results of our calculations with the experimental data for  $^{10}$ B and  $^{14}$ N. First one can see from figures and the dashed red distributions decreases faster than the black distributions with increasing q. This is attributed to the charge density pulls out due to the addition of neutrons to  $^{10}$ B and  $^{14}$ N and thus the form factors decrease with increasing q. In this work, the  $\sigma_R$  of the exotic  $^{14}$ B and  $^{18}$ N nuclei on target  $^{12}$ C are studied by the KF and GM with the OLA and summarized in **Table 5** along with experimental results (42). The HO densities are used in GM calculations. It is demonstrated that the experimental data satisfactorily well by our calculations obtained by GM while the extracted  $\sigma_R$  by Kox formula closely agree with those experimental data within quoted error.

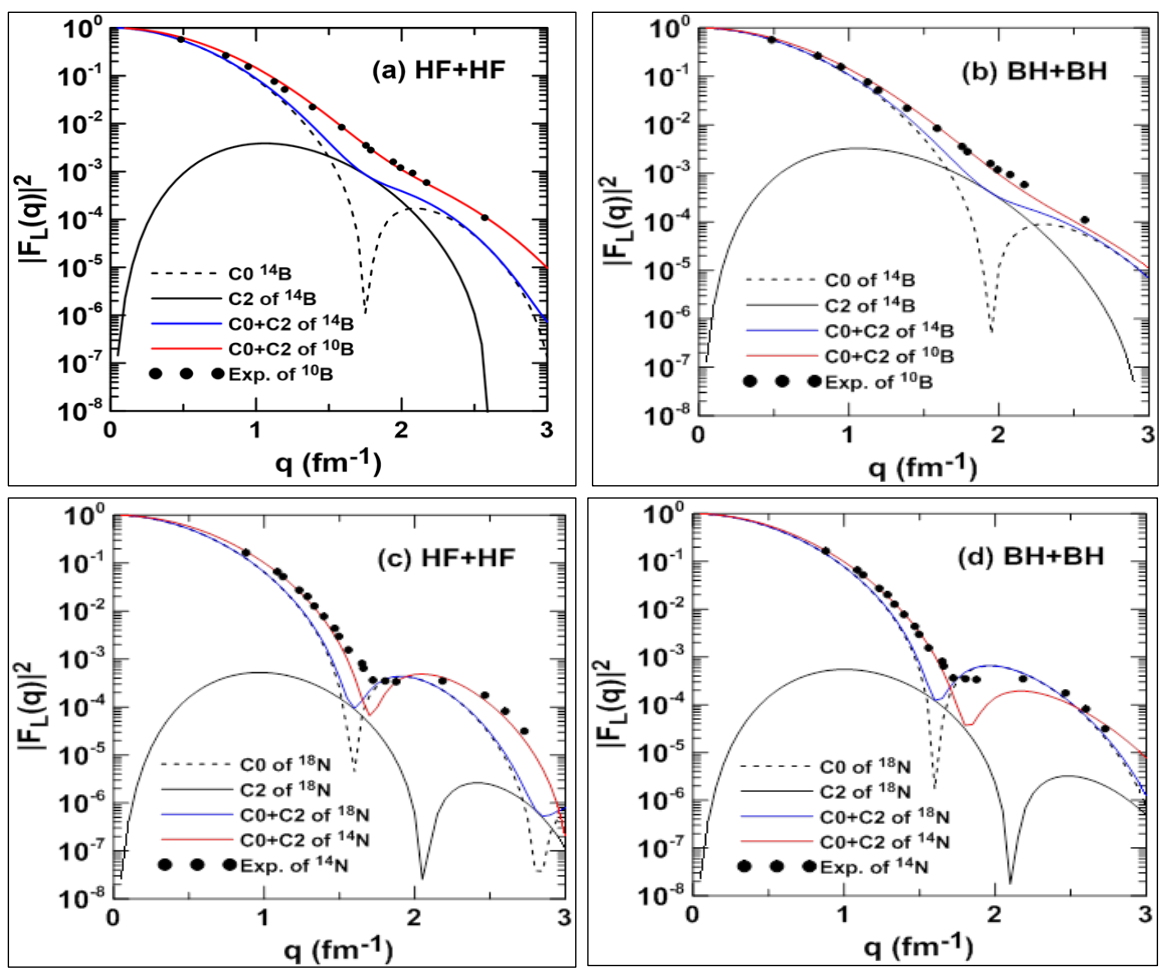


Figure 4. The longitudinal form factors of isotopes <sup>10,14</sup>B and <sup>14,18</sup>N.

**Table 5.** The reaction cross sections of the exotic <sup>14</sup>B and <sup>18</sup>N nuclei on target <sup>12</sup>C.

Halo nuclei	Energy (MeV) (42)	$\sigma_R$ (Cal.	) (mb)	$\sigma_R$ (Exp.) (mb) (42)
Halo nuclei	Energy (MeV) (42)	KF	GM	O <sub>R</sub> (Exp. ) (IIII) (42)
<sup>14</sup> B	790	961	937	929±26
<sup>18</sup> N	1020	1.077	1062	1046±8

The Q and  $\mu$  moments for  $^{10,14}$ B and  $^{14,18}$ N isotopes are calculated in psd-model space using PSDMK interaction (43) and tabulated in Table 6 together with the experimental data (44). The effective charges of NuShellX@MSU code (NS)  $\left(e_p^{eff}=1.5, e_n^{eff}=0.5e\right)$  and free-nucleon g factors have been used to evaluate the Q and  $\mu$  moments, respectively. In general, the theoretical and experimental results of Q and  $\mu$  moments agree reasonably for all selected nucleus.

**Table 6.** Calculated and experimental results of Q and  $\mu$  moments.

Nuclei	Q	Exp. (44)	μ	Exp. (44)
<sup>14</sup> B	4.45	2.98±0.008	0.986	1.18±0.005
$^{10}\mathrm{B}$	9.07	$8.47 \pm 0.006$	1.82	$1.80\pm0.006$
$^{18}N$	1.97	$2.70\pm0.004$	-0.107	$-0.135 \pm 0.015$
$^{14}N$	1.08	1.93±0.008	0.333	$0.403 \pm 0.006$

#### 4. Conclusion

The ground-state properties like the nuclear densities and the rms radii for exotic neutron-rich nuclei <sup>14</sup>B and <sup>18</sup>N have been investigated in the framework of the HF and BH calculations. This study draws the following conclusions:

The evaluated results are compared with available experimental data. It is found that both the HF and BH calculations are capable of providing theoretical predictions on the structure of exotic nuclei (considered in this study) and provide a satisfactory description of experimental data.

The halo structure of the above exotic nuclei is emphasized through exhibiting the long tail performance in their calculated matter density distributions, where this performance is considered a distinctive feature of halo nuclei.

It is found that the major difference between the calculated form factor of unstable nuclei (<sup>14</sup>B, <sup>18</sup>N) and those of stable nuclei (<sup>10</sup>B, <sup>14</sup>N) is attributed to the charge density pulls out due to the addition of neutrons to <sup>10</sup>B and <sup>14</sup>N, and thus the form factors decrease with increasing q. The calculated results of the reaction cross sections using the Kox formula and the Glauber model with an optical limit approximation are in good agreement with experimental data at high energy. The calculated results of the nuclear magnetic dipole and electric quadrupole moments using the Shell model calculations within the two-body effective interactions are in reasonable agreement with experimental data.

### Acknowledgment

The researchers are very grateful to Prof. Dr. Alex Brown for his code (NuShellX@MSU code).

#### **Conflict of Interest**

The authors declare that they have no conflicts of interest.

#### **Funding**

The article was done depending on self-fund and no establishments supplied us.

#### **Ethical Clearance**

The work and calculations were accomplished using the NuShellX@MSU code

#### References

- 1. Dobrovolsky AV, Korolev GA, Inglessi AG, Alkhazov GD, Colò G, Dillmann I.Nuclear-matter distribution in the proton-rich nuclei <sup>7</sup>Be and <sup>8</sup>B from intermediate energy proton elastic scattering in inverse kinematics. Nucl Phys A. 2019;989:40–58. https://doi.org/10.1016/j.nuclphysa.2019.05.012
- 2. A. N. Antonov, D. N. Kadrev, M. K. Gaidarov, E. Moya de Guerra, P. Sarriguren, J. M. Udias, V. K. Lukyanov, E. V. Zemlyanaya, and G. Z. Krumova. Charge and matter distributions and form factors of light, medium, and heavy neutron-rich nuclei. Phys. Rev. C 72, 2005, 044307 1-11. https://doi.org/10.1103/PhysRevC.72.044307
- 3. Noori RI, Ridha AR. Density Distributions and Elastic Electron Scattering Form Factors of Proton-rich <sup>8</sup>B, <sup>17</sup>F, <sup>17</sup>Ne, <sup>23</sup>Al and <sup>27</sup>P Nuclei. Iraqi J Sci. 2019;60(6):1286-1296. https://doi.org/10.24996/ijs.2019.60.6.12
- 4. C.A. Bertulani. Probing nuclear skins and halos with elastic electron scattering. J.Phys.G34. 2007. 315-334. https://doi.org/10.1088/0954-3899/34/2/011
- 5. Tanihata I, Hamagaki H, Hashimoto O, Shida Y, Yoshikawa N. Measurements of interaction cross sections and nuclear radii in the light p-shell region. Phys Rev Lett. 1985;55:2676.: <a href="https://doi.org/10.1103/PhysRevLett.55.2676">https://doi.org/10.1103/PhysRevLett.55.2676</a>
- 6. Fukuda M, Ichihara T, Inabe N, Kubo T, Kumagai H. Neutron halo in <sup>11</sup>Be studied via reaction cross sections. Phys Lett B. 1991;268:339.

- 7. Nakamura T, Fukuda N, Kobayashi T, Aoi N, Iwasaki H. Coulomb dissociation of <sup>19</sup>C and its halo structure. Phys Lett B. 1999;83:1112.
- 8. Blank B, Marchand C, Pravikoff MS, Baumann T, Boué F. Total interaction and proton-removal cross-section measurements for the proton-rich isotopes <sup>7</sup>Be, <sup>8</sup>B, and <sup>9</sup>C. Nucl Phys A. 1997;624:242. <a href="https://doi.org/10.1016/S0375-9474(97)81837-4">https://doi.org/10.1016/S0375-9474(97)81837-4</a>
- 9. Ilieva S, Aksouh F, Alkhazov GD, Chulkov LV. Nuclear-matter density distribution in the neutron-rich nuclei <sup>12</sup>, <sup>14</sup>Be from proton elastic scattering in inverse kinematics. Nucl Phys A. 2012;875:8.
- 10. Tanihata I, Kobayashi T, Yamakawa O, Shimoura S, Ekuni K. Measurement of interaction cross sections using isotope beams of Be and B and the isospin dependence of the nuclear radii. Phys Lett B. 1988;206:592. https://doi.org/10.1016/0370-2693(88)90702-2
- 11.Geithner W, Kappertz S, Keim M, Lievens P, Neugart R. Measurement of the Magnetic Moment of the One-Neutron Halo Nucleus <sup>11</sup>Be. Phys Rev Lett. 1999;83:3792. https://doi.org/10.1103/PhysRevLett.83.3792
- 12. Alkhazov GD, Belostotsky SL, Vorobyov AA. Scattering of 1 GeV protons on nuclei. Phys Rep. 1978;42:89.https://doi.org/10.1016/0370-1573(78)90083-2
- 13. Dobrovolsky AV, Alkhazov GD, Andronenko MN, Bauchet A, Egelhof P. Study of the nuclear matter distribution in neutron-rich Li isotopes. Nucl Phys A. 2006;766:1. <a href="https://doi.org/10.1016/j.nuclphysa.2005.12.004">https://doi.org/10.1016/j.nuclphysa.2005.12.004</a>.
- 14.Rahi SA, Flaiyh GN. Matter Density Distributions, Root-mean Square Radii and Elastic Electron Scattering Form Factors of Some Exotic Nuclei (17B, 11Li, 8He). Iraqi J Phys. 2021;19(50):60-69. https://DOI: 10.30723/ijp.v19i50.675.
- 15.Masaru Hongo, Dam Thanh Son. Universal Properties of Weakly Bound Two-Neutron Halo Nuclei. Phys. Rev. Lett. 128, 212501 (2022). https://doi.org/10.1103/PhysRevLett.128.212501
- 16.Mohammed R A, Majeed W Z. Exotic Structure of 17Ne-17N and 23Al-23Ne Mirror Nuclei. East Eur J Phys. 2022;4:72-79. https://doi.org/10.26565/2312-4334-2022-4-05.
- 17. Abdullah AN. The neutron halo structure of <sup>14</sup>B, <sup>22</sup>N, <sup>23</sup>O and <sup>24</sup>F nuclei studied via the generalized Woods-Saxon potential. Pramana J Phys. 2020;94:154. <a href="https://doi.org/10.1007/s12043-020-02011-x">https://doi.org/10.1007/s12043-020-02011-x</a>.
- 18. Abdullah AN. Nuclear matter distributions of neutron-rich <sup>4</sup>He, <sup>6</sup>Li, <sup>14</sup>Be and <sup>7</sup>Be halo nuclei studied by the Bear Hodgson potential. Mod Phys Lett A. 2020;35:2050212. https://doi.org/10.1142/S0217732320502120.
- 19.Ridha A R, Abbas Z M. Theoretical Study of Density Distributions and Size Radii of 8B and 17Ne. Iraqi J Sci. 2018;59(2C):1046-1056. https://doi.org/10.24996/ijs.2018.59.2C.8.
- 20.Zhang HB, Zhao TC, Xu ZG, Wang Y, Chen RF, Huang TH, Gao H, Jia F, Fu F, Gao Q, Han JL, Zhang XH, Zheng C, Yu YH, Fan RR, Li B, Guo ZY. Configuration of the valence neutrons of ^17B. *Chin Phys C*. 2008;32(7):548-551. https://doi.org/10.1088/1674-1137/32/7/007.
- 21.Rahi SA, Flaiyh GN. Study of matter density distributions, elastic electron scattering form factors and root mean square radii of 9C, 12N, 23Al, 11Be and 15C exotic nuclei. Iraqi J Sci. 2022;63(3):1018–1029. https://doi.org/10.24996/ijs.2022.63.3.11.
- 22.Bear K, Hodgson PE. The systematics of nuclear bound states. J Phys G Nucl Phys. 1978;4(12):L287. <a href="https://doi.org/10.1088/0305-4616/4/12">https://doi.org/10.1088/0305-4616/4/12</a>.
- 23.Blocki JP, Feldmeier H, Swiatecki WJ. Dynamical hindrance to compound-nucleus formation in heavy-ion reactions. Nucl Phys A. 1986;459:77. https://doi.org/10.1016/0375-9474(86)90061-8.
- 24.Reinhard PG, Hummer F, Goeke K. Matter density distributions and elastic form factors of some two-neutron halo nuclei. Z Phys A. 1984;317:339. https://www.ias.ac.in/article/fulltext/pram/089/03/0043
- 25.Qiang LG. A systematic study of nuclear properties with Skyrme forces. J Phys G Nucl Part Phys. 1991;17:1. https://doi.org/10.1088/0954-3899/17/1/002.

- 26.Ridha AR, Abbas ZM. Study of matter density distributions, elastic charge form factors and size radii for halo 11Be, 19C and 11Li nuclei. Iraqi J Phys. 2018;16(36):29–38. https://doi.org/10.30723/ijp.v16i36.23.
- 27.Baldık R, Aytekin H, Tel E. Investigation of neutron and proton distributions of He, Li and Be isotopes using the new Skyrme-force parameters. Phys Atom Nucl. 2010;73:74. <a href="https://ui.adsabs.harvard.edu/abs/2010PAN...73...74B">https://ui.adsabs.harvard.edu/abs/2010PAN...73...74B</a>.
- 28.Antonov AN, Gaidarov MK, Kadrev DN, Hodgson PE, Moya de Guerra E. Charge density distributions and related form factors in neutron-rich light exotic nuclei. Int J Mod Phys E. 2004;13:759–772. https://doi.org/10.1142/S0218301304002430.
- 29.Zheng T, Yamaguchi T, Ozawa A, Chiba M, Kanungo R. Study of halo structure of <sup>16</sup>C from reaction cross section measurement. Nucl Phys A. 2002;709:103. <a href="https://doi.org/10.1016/S0375-9474(02)01043-6">https://doi.org/10.1016/S0375-9474(02)01043-6</a>
- 30.Kox S, Gamp A, Perrin C, Arvieux J, Bertholet R. Trends of total reaction cross sections for heavy ion collisions in the intermediate energy range. Phys Rev C. 1987;35:1678. https://doi.org/10.1103/PhysRevC.35.1678
- 31.Shlomo S. Modern energy density functional for nuclei and the nuclear matter equation of state. Phys Atom Nucl. 2010;73:1390–1397. https://doi.org/10.1134/S1063778810080120
- 32.Brown BA, Rae WDM. The Shell-Model Code NuShellX@MSU. Nucl Data Sheets. 2014;120:115. https://doi.org/10.1016/j.nds.2014.07.022
- 33. Wang M, Audi G, Kondev FG, Huang WJ, Naimi S, Xu X. The AME2016 atomic mass evaluation (II). Chin Phys C. 2017;41:030003.
- 34.Ahmad S, Usmani A, Khan Z. Matter radii of light proton-rich and neutron-rich nuclear isotopes. Phys Rev C. 2017;96:064602. https://doi.org/10.1103/PhysRevC.96.064602
- 35.Tanaka M, Fukuda M, Nishimura D, Suzuki S, Takechi M. Reaction cross sections for <sup>8</sup>He and <sup>14</sup>B on proton target for the separation of proton and neutron density distributions. JPS Conf Proc. 2015;6:020026. https://inspirehep.net/literature/1389288
- 36.Estradé A, Kanungo R, Horiuchi W, Ameil F, Atkinson J. Proton radii of <sup>12</sup>—<sup>17</sup>B define a thick neutron surface in <sup>17</sup>B. Phys Rev Lett. 2013;113:132501. https://doi.org/10.1103/PhysRevLett.113.132501
- 37.Liatard E, Bruandet JF, Glasser F, Kox S, Chan TU. Matter distribution in neutron-rich light nuclei and total reaction cross-section. Europhys Lett. 1990;13:401. <a href="https://doi.org/10.1209/0295-5075/13/5/004">https://doi.org/10.1209/0295-5075/13/5/004</a>
- 38.Fukuda M, Nishimura D, Suzuki S, Tanaka M, Takechi M. Neutron halo in <sup>14</sup>B studied via reaction cross sections. EPJ Web Conf. 2014;66:02037. https://doi.org/10.1051/epjconf/20146602037
- 39.Ozawa A. Measurement of the interaction cross-section and related topics. Eur Phys J A. 2002;13:163. https://doi.org/10.1140/epja1339-30
- 40.Stovall T, Goldenberg J, Isabelle DB. Study of <sup>27</sup>Al by elastic electron scattering. Nucl Phys. 1966;86:225. DOI not available. <a href="https://inspirehep.net/literature/1432054">https://inspirehep.net/literature/1432054</a>
- 41.Dally EB, Croissiaux MG, Schweitz B. Scattering of high-energy electrons by nitrogen-14 and -15. Phys Rev C. 1970;2:2057. https://doi.org/10.1103/PhysRevC.2.2057
- 42.Ozawa A, Suzuki T, Tanihata I. Nuclear size and related topics. Nucl Phys A. 2001;693:32–62. <a href="https://doi.org/10.1016/S0375-9474(01)01152-6">https://doi.org/10.1016/S0375-9474(01)01152-6</a>
- 43.Millener DJ, Kurath D. The particle-hole interaction and the beta decay of <sup>14</sup>B. Nucl Phys A. 1975;255:315–338. https://doi.org/10.1016/0375-9474(75)90683-1
- 44. Stone NJ. Table of nuclear magnetic dipole and electric quadrupole moments. INDC(NDS)–0658. IAEA; 2014. https://www-nds.iaea.org/publications/indc/indc-nds-0658.pdf